Utilizing metaheuristic optimization with transfer learning for efficient colorectal carcinoma detection in biomedical imaging

Lova Naga Babu Ramisetti[1], Desidi Narsimha Reddy[2], Harikrishna Pathipati[3], Yenumula Srividya[1], Swetha Pesaru[1]

[1]Department of Information Technology, Vignana Bharathi Institute of Technology, Hyderabad, India
[2]Data Consultant (Data Governance, Data Analytics: Enterprise Performance Management, AI&ML), Soniks Consulting LLC, Dallas, United States
[3]Department of Information Technology, ITG Technologies, Houston, United States

Article Info

ABSTRACT

Colorectal cancer (CRC) is the third most popular cancer across the world. Its morbidity and death are reduced by early screening and detection. The screening outcomes are enhanced by computer-aided detection (CAD) and artificial intelligence (AI) in screening models. Contemporary imaging technologies such as near-infrared (NIR) fluorescence and optical coherence tomography (OCT) are implemented to identify the early-phase CRC of the gastrointestinal tract (GI tract) via the identification of morphological and microvasculature changes. Most recently, deep learning (DL)-based approaches have been used directly on raw data. Nevertheless, they are hampered by biomedical data deficiency. These studies can enhance metaheuristic optimization using the transfer learning to detect colorectal cancer successfully (MHOTL-ECRCD). The MHOTL-ECRCD method concentrates on biomedical imaging of CRC categorization and detection. MHOTL-ECRCD minimizes noise through the process of adaptive bilateral filtering (ABF). In MHOTL-ECRCD methodology, Inception-ResNet-V2 is adopted to learn the inherent and complicated image preprocessing features thus used during feature extraction. To classify CRC and detect it, the gated recurrent unit (GRU) approach is applied. Lastly, parameters of the GRU model are optimized with a human evolutionary algorithm. Good classification results of MHOTL-ECRCD are demonstrated by a number of benchmark dataset trials. MHOTL-ECRCD technology superseded the recent techniques as large volumes of comparison were made.

This is an open access article under the CC BY-SA license.

Corresponding Author:

Desidi Narsimha Reddy
Data Consultant (Data Governance, Data Analytics: Enterprise Performance Management, AI&ML)
Soniks Consulting LLC
Dallas, United States
Email: dn.narsimha@gmail.com

1. INTRODUCTION

Global cancer data from 2018 showed that the occurrence of colorectal cancer (CRC) ranked highest later breast and lung cancer, and globally, it represents almost 10% per annum cancer patients amongst either men or women [1]. While people aged 65 years and above maximum number of victims of these disorders, the danger of young patients is equally important, with the maximum possibility because of heredity (35%) followed by other reasons like poor nutritional habits, smoking, and obesity [2]. This rate shows no development toward failure but instead is predicted to improve by more than 60% in the following years, with more than two million newly diagnosed and over a million demises by the next several years.

Consequently, been an observed requirement for developing an optimum diagnosis tactic for the earlier and more accurate recognition of CRC patients [3]. The present performance and treatment of CRC depends on conventional imaging techniques; namely computed tomography (CT), magnetic resonance imaging (MRI), positron emission tomography (PET), optical coherence tomography (OCT), and conventional colonoscopy [4]. The current model for CRC screening is colonoscopy, which is based exclusively on the doctor's experience and judgment. During colonoscopy, the gained abnormal tissue should be propelled for pathological inspection for diagnosing the diseases. In addition, colonoscopy, the above-mentioned MRI, PET, and CT are the traditional diagnostic imaging conditions for CRC detection [5]. OCT provides micrometer resolution and is verified to be best for cancer imaging. Nevertheless, it has restrictions owing to annoying higher optical scattering within the tissue [6]. CT is a non-invasive technology and offers 3D tomographic images of the complete colon. CT has been improved at detecting small lesions (lower than 1 cm in size) in comparison with MRI [7].

The improvement of computer-aided detection (CAD) methods for CRC is dated from the classic approaches, which need composite a deductive mathematics knowledge developed machine learning (ML)-based techniques, which are capable of performing above human accuracy levels [8]. Even though cancer analysis with deep learning (DL) is a most prevalent interest area within the medical imaging sector, wide-ranging literature assessments covering different features of CRC diagnosis and prediction using new DL models are always limited. The present reviews limited surveys depending on different categories of convenient standard CRC imaging datasets [9]. Additionally, in a limited period, there have been ample new investigations and discoveries from DL-based CRC diagnosing. An appropriate analysis of these modern outcomes regarding adapted data pre-processing approaches has been required, and the techniques requested are to be advanced to facilitate future investigators and researchers in this domain [10]. CRC ranks as the third most diagnosed cancer globally, leading to significant morbidity and mortality. Early detection through effective screening is critical for improving patient outcomes. However, the current screening methods often face challenges such as variability in detection rates, reliance on human interpretation, and limitations in imaging techniques. The integration of advanced technologies such as CAD and artificial intelligence (AI) has shown promise in enhancing CRC screening outcomes. Nonetheless, the utility of these technologies is hindered by the scarcity of annotated data in the biomedical field, necessitating the development of more efficient detection techniques that can leverage existing data effectively.

These studies grow a metaheuristic optimization with transfer learning for efficient colorectal carcinoma detection (MHOTL-ECRCD) technique. In the MHOTL-ECRCD technique, the adaptive bilateral filtering (ABF) model is used for noise reduction. For feature extraction, the MHOTL-ECRCD technique applies the Inception-ResNet-V2 method for learning the intrinsic and complex features of the image preprocessing. Moreover, the gated recurrent unit (GRU) technique is used for the classification and detection of the CRC. Finally, the parameter tuning of the GRU technique is performed by the use of a human evolutionary optimization algorithm (HEOA). To demonstrate the good classification outcome of the MHOTL-ECRCD technology, a broad variety of experiments occurs from the benchmark dataset.

2. LITERATURE SURVEY

Peng and Deng [11] present a CRC monitoring and diagnosis background, then execute a scientific study on the medical imaging AI of CRC monitoring and diagnosis and ML, and lastly outline it together with the innovative computing intelligence method for the application of safe medical imaging. Oswald *et al.* [12] created a new fluorescence excitation-HSI method for spectroscopic data and model images concurrently over the platform of endoscope and microscope to improve the possibility of diagnosis. Regrettably, fluorescence excitation scanning HSI datasets present the main challenges for processing the data, classification, and interpretability owing to their higher dimension. The advanced AI method can execute the recent classification of HSI with classification performance/various speed balances by modifying the dataset dimensionality, assisting various DL model dimensions, and changing the DL model structure. Tang *et al.* [13] present a novel technique named MGCNet that uses multi-series MRI to predict 1-year recurrence-free and recurrence existence in patients afterward the resection of CRLM. In redundancy and complexity light of features in the liver area, the author created the multi-modal managed local feature fusion component to use the feature of cancer to lead the dynamic fusion of prognostically related local features in the liver. Alternatively, to resolve the spatial data loss in the fusion of multi-sequence MRI, the cross-modal corresponding exterior attention unit created an exterior mask division to create the correlation of inter-layer.

Zidan *et al.* [14] present a new technique called the SwinCup method for histopathology image segmentation. The author utilizes a hierarchical Swin transformer with shifted windows as encoding for extracting the context features globally. The multi-scale feature extraction in a Swin transformer allows the method to assist the various regions within the image at various scales. A cascaded-up sampling decoding is

utilized by an encoding to enhance its feature aggregation. Lavinia and Sahafi [15] introduce an AI-based polyp detection method utilizing the YOLO-V8 system. To perform extensive evaluations, a diverse dataset was created from many freely accessible resources. It exceeded additional advanced methods regarding the precision of mean average. YOLO-V8 s presented an offset among computational and precision efficacy. Our study offers useful information for developing the polyp recognition and gives to the development of CAD for CRC.

Muneer *et al.* [16] presented 2 methods, radiomic-based support vector machine (SVM) and a DL method to identify various kinds of cells in CRC utilizing pathological images. In initial method, the features of radiomics have been removed from the HI and SVM utilized for the CRC classification. The next method extracted the features of DL and identified the CRC by utilizing Res-Net-18. The research used a dataset of 5000 CRC pathological images, with 8 cell class labels to be identified. Sabol *et al.* [17] introduced an explainable classifier for making decision support for clinical assessment. The presented method does not offer a description regarding the connection between the decisions and the input, nevertheless provides a human-friendly clarification regarding the decision plausibility. CFCMC describes its decisions in 3 techniques: over a semantic description regarding the misclassification possibilities, presenting the training instances answerable for a particular prediction, and presenting training instances from differing class labels. In this study, the author describes the numerical architecture of the classification that is not intended to be utilized as a completely automatic diagnosis device but as a helping method for medical professionals. The contributions of the MHOTL-ECRCD technique are as follows:

−   Enhanced detection and classification: the technique significantly improves the classification and detection of CRC through advanced methodologies, leading to better screening outcomes.
−   Noise reduction: by incorporating the ABF model, the technique effectively reduces noise in biomedical imaging, which is crucial for accurate diagnosis.
−   Feature extraction: the use of the Inception-ResNet-V2 method for feature extraction allows for the learning of intrinsic and complex features from images, enhancing the model's ability to identify CRC in its early stages.
−   Application of advanced algorithms: the integration of GRU techniques for classification and detection provides a robust framework for handling the complexities of CRC detection.
−   Parameter optimization: the implementation of a HEOA for parameter tuning of the GRU model ensures optimal performance and accuracy in classification tasks.
−   Benchmarking and validation: the extensive experiments conducted on benchmark datasets validate the effectiveness of the MHOTL-ECRCD technique, demonstrating its superiority over recent methods in terms of classification outcomes.
−   Contribution to biomedical imaging: this work advances the field of biomedical imaging by combining CAD and AI, paving the way for future research and development in CRC screening technologies.
−   Potential for broader applications: the methodologies developed can potentially be adapted for other types of cancers or medical imaging challenges, broadening the impact of this research beyond CRC.

3. METHOD

In this article, we have advanced a new MHOTL-ECRCD technique. The MHOTL-ECRCD technology mostly concentrates on the classification and detection of CRC utilizing biomedical imaging. It contains four various kinds of stages involving image preprocessing, feature extraction, classification, and parameter selection are demonstrated in Figure 1.

3.1. Stage I: image preprocessing

Initially, the MHOTL-ECRCD technique takes place ABF model is used for the noise reduction. ABF is a great technology for improving biological images, mostly in the CRC detection context [18]. Utilizing the intensity and spatial image information, these methods efficiently smooth areas of related intensities while protecting the edges that are serious in detecting cancerous tissues. The flexible nature of the filter permits it to adjust the filter parameters dynamically depending on the characteristics of a local image, guaranteeing that significant features are preserved. These methods can considerably increase the clarity and contrast of colorectal images, making it easy for medical specialists to diagnose and detect cancerous developments. Eventually, ABF improves diagnostic accuracy and assists in improved medical results in CRC screening.

3.2. Stage II: feature extraction

For feature extraction, the MHOTL-ECRCD technique applies the Inception-ResNet-V2 method for learning the intrinsic and complex features from the image preprocessing. The benefit of the InceptionResNet-v2 architecture model is its capacity to recognize objects with greater precision and handle

unstructured data by related feature extraction from images using convolution [19]. Whereas convolution implementation image extraction to gain a method in the kernel matrix form. During this process, filtration can be performed that moves with a particular "step value" on an image input. Our implementation of expression at the parameter value regulates how much filter transfers in the input image. Additionally, the convolution results became inputs for the fully connected elements for the process of classification.

The InceptionResNetV2 architecture joins initial and residual connection techniques to increase performance. This hybrid model permits the network to take benefit of the assistances of both methods, comprising quicker times of training and preventing disappearing gradient problems. Residual connections also permit the network to pass over several layers throughout training. Additionally, InceptionResNetV2 utilizes a dual-sized kernel in a particular layer to draw patterns with different hierarchical, which also increases the network's capability to capture features of different complexities. This Inception-ResNetV2 method has various blocks, which have rectified linear unit (ReLU) activation functions, convolutional layers, ResNet, filter merging, and the original structure. The unique design of the Inception-ResNetV2 technique and the efficient filter usage has resulted in inspiring outcomes in the medicinal imaging classification task. Therefore, we utilized the Inception-ResNetV2 pre-trained approach as the basis for this paper.

The Inception-ResNet-v2 model has been regularly applied for CT-scan image classification because of its capability to extract significant features from healthcare images. This DL architecture associations two renowned methods such as ResNet and Inception. The Inception model outshines feature extraction at numerous scales, whereas ResNet efficiently responds to the vanishing gradients problem during training. The Inception-ResNet-v2 model has been designed to overwhelm the limitations of these two method and attain higher accuracy in tasks of image classification. Furthermore, these approaches are real in controlling larger datasets and decreasing computational time.
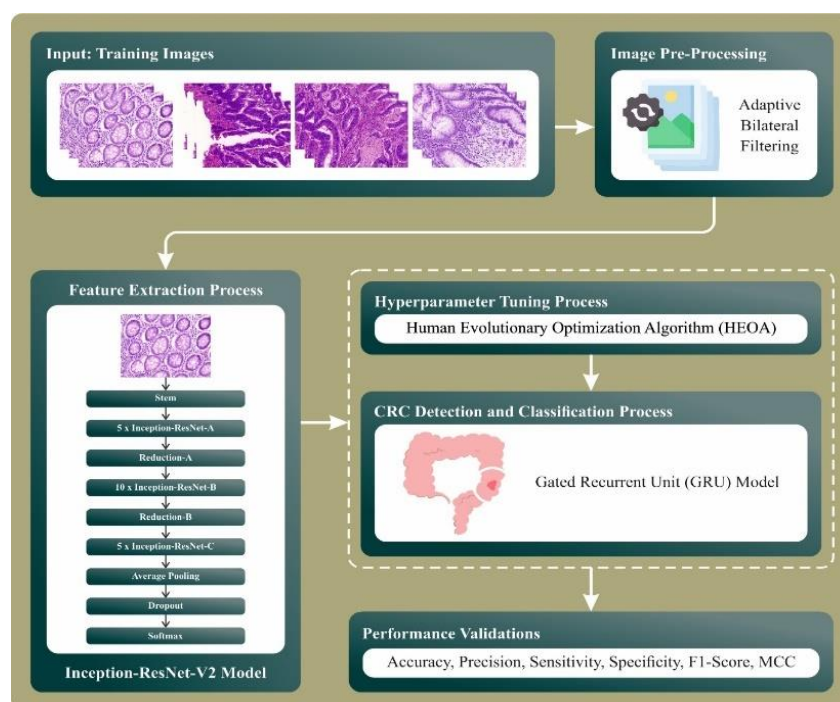

Figure 1. Workflow of MHOTL-ECRCD technique

3.3. Stage III: CRC detection using GRU

At this stage, the GRU method is used for the classification and detection of the CRC. GRU is an advanced recurrent neural network (RNN) architecture [20]. Like the RNN growths, GRU contains the capacity to deal with gradient exploding and vanishing gradient difficulties. A vanishing gradient follows after the computed gradient turns into so smaller since the GRU architecture is so intricate that the gradient should get over longer sequences. In the meantime, the gradient explodes while the gradient grows progressively larger which causes the process of training to be lengthened. GRU has small parameters and weights, hence the time requisite in the process of training should be quicker and give a smaller value of error. GRU has greater performance on serial complications, with image classification, natural language

processing (NLP), and prediction of time-sequence. GRU possesses dual gates such as the reset and the update gates. The update gate can be employed to define several previous pieces of information that will remain saved and recollect novel information. Whereas the reset gate is applied to associate original input and previous information and decide whether the innovative information will be forgotten or not. Figure 2 represents the structure of GRU.

The procedure within the GRU gated architecture begins by joining the hidden layer (HL) at the earlier time (h_{t-1}) as well as input value at time $t(x_t)$ to make the value of output (y_t). These formulations of the GRU-gated framework have been expressed below:

$$z_t = ReLU(W_z\,[h_{t-1}, x_t]) \tag{1}$$

$$r_t = ReLU(W_r\,[h_{t-1}, x_t]) \tag{2}$$

$$\tilde{h}_t = ReLU\big(W_{\tilde{h}} \cdot (r_t * h_{t-1}, x_t)\big) \tag{3}$$

$$\tilde{h}_t = ReLU\big(W_{\tilde{h}} \cdot (r_t * h_{t-1}, x_t)\big) \tag{4}$$

$$h_t = (1 - z_t) * h_{t-1} + z_\tau * \tilde{h}_t \tag{5}$$

$$y_t = ReLU(W_o \cdot h_t) \tag{6}$$

whereas, z_t: updated gate, r_t: gate of reset, $\tilde{h}_t$: candidate HL, h_{t-1}: HL on the earlier time, h_t: the present upgraded HL, W_z: weighted matrix on an updated gate, W_r: weighted matrix on the gate of reset, $W_{\tilde{h}}$: weighted matrix on candidate HL, W_o: weighted matrix of input values at a timing t, x_t: input at a timing t, and y_t: output as of the time t.

According to the formulations of the gated GRU architecture, there is an equations of updated gate z_t, gated reset r_t, candidate HL $\tilde{h}_t$, HL h_t, and output y_t. During formulations z_t and r_t, $[h_{t-1}, x_t]$ represent vector concatenation h_{t-1} and x_t vector. x_t the vector contains a size of n by the vector form x_t stands $[x_1, x_2, \dots, x_n]$. h_{t-1} a vector as magnitude m using the vector form h_{t-1} is $[h_1, h_2, h_3, \dots, h_m]$. This complex vector $[h_{t-1}, x_t]$ indefinite size $m + n$ by the form $[h_1, h_2, h_3, \dots, h_m, x_1, x_2, \dots, x_n]$. $W_Z, W_r, W_{\tilde{h}}$, and W_o signifies weighted matrices by the updated gate, gate of reset, candidate HL, and output with size $(u, m + n)$. The u value represents the neuron-numbered elements of the GRU structure, whereas m and n denote vector magnitude h_{t-1} and x_t. $\cdot$ characterizes the operation of matrix multiplication. This symbol $*$ signifies the element-to-element operation of multiplication that can be a mathematical process among two matrices or vectors where every component at the equivalent location is multiplied by one another.
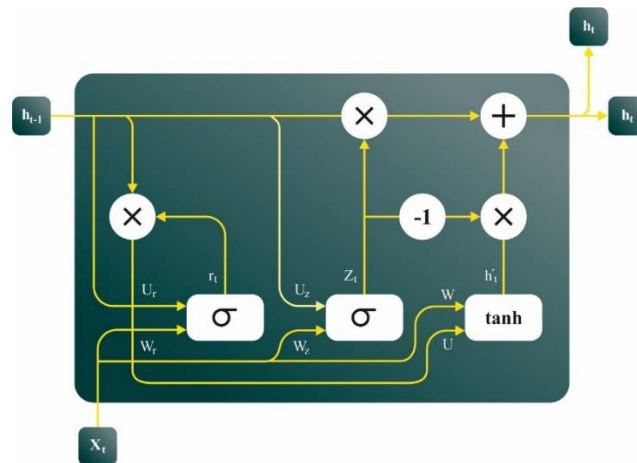

Figure 2. GRU architecture

3.4. Stage IV: parameter selection

Finally, the parameter tuning of the GRU approach can be made by the use of HEOA. The HEOA is a meta-heuristic technique, which is stimulated by human development [21]. HEOA splits the global search method into dual different stages such as human development and human exploration. Use logical chaos map

for initialization. Separating the optimization stage into phases of human exploration and development, the early global search was executed in the initial stage. Its mathematical expression is exposed in (7):

$$X_i^{t+1} = \beta \left(1 - \frac{t}{\text{Max}_{iier}}\right)(X_i^t - X_{best})Levy(\text{dim}) +$$
$$X_{best}\left(1 - \frac{t}{\text{Max}_{iter}}\right) + (X_{mean}^t - X_{best})floor\left(\frac{rand}{iump}\right)jump \qquad (7)$$

whereas, β refers to function of adaptive, and dim represents the problem dimension. X_i^t signifies the present location, while X_i^{t+1} means the location of the subsequent update. X_{best} relates to the finest location discovered so far, and X_{mean}^t denotes the average location in the present population. $Levy$ signifies the Levy distribution, and f_{jump} is the coefficient of jump.

In the 2nd stage, the population is classified into leaders, losers, explorers, and followers, utilizing a dissimilar searching tactic. The numerical formulation of the leader was definite in (8).

$$X_i^{t+1} = \begin{cases} \omega X_i^t \exp\left(\frac{-t}{randn \cdot \text{Max}_{iter}}\right), R < A \\ \omega X_i^t + Rn \cdot ones(1, dim), R \geq A \end{cases} \qquad (8)$$

Here, $randn$ is a randomly produced number in the interval of [0,1]. The function ones $(1, dim)$ produces a rowed vector, whereas every element can be fixed to 1. Rn means a randomly generated value that signifies the intricacy of the condition linked with the leaders. $A = 0.6$ represents the calculation state value. The knowledge acquisition alleviates co-efficient is signified as ω, which slowly declines the progress of development.

HEOA is an effective search function, but its transition method amongst dual phases is very easy and could be improved further. The evolutionary ways of dissimilar phases of human evolution must be diverse and complex, therefore this study accepts the lens opposition-based learning to increase the learning capability and complexity of the transition method. While x takes 0 as the baseline point for getting its equivalent opposite point x^* that could be gained from standard lens imaging. Assume $k = h/h^*$ for obtaining (9) depends upon lens opposition-based learning.

$$X_i^* = (k + 1)(a_i + b_i)/2k + X_i/k \qquad (9)$$

Here, X_i denotes original location and X_i^* means opposite solution. b_i and a_i represents least and highest limits within the space of searching. Every enhanced position by the HEOA is enlarged utilizing (9) to increase the searchability. The HEOA progresses a fitness function (FF) for reaching superior performance of classification. It states a positive integer to illustrate the better performance of the candidate solutions. In this article, the classification rate of error minimization can be determined for FF, as specified in (10).

$$fitness(x_i) = ClassifierErrorRate(x_i)$$
$$= \frac{number\ of\ misclassified\ samples}{Total\ number\ of\ samples} * 100 \qquad (10)$$

4. RESULT ANALYSIS AND DISCUSSION

In this article, the performance validation analysis of the MHOTL-ECRCD technique is examined with Warwick-QU database [22], [23]. The dataset contains 165 instances with two class labels described in Table 1. Figure 3 presents the classification results of the MHOTL-ECRCD technique from the test database. Figures 3(a) and (b) exhibitions the confusion matrix using correct identification and classification of each 2 class labels on a 70:30 TRAP/TESP. Figure 3(c) illustrates the study of PR, demonstrating higher values across each class. At last, Figure 3(d) explains the investigation of ROC, portraying efficient results with higher ROC values for various classes.

Table 1. Details of dataset

Classes	Image count
Benign tumor	74
Malignant tumor	91
Total images	165

In Table 2, the CRC detection results of MHOTL-ECRCD technique under 70%TRAP and 30%TESP are clearly defined. The outcomes implied that the MHOTL-ECRCD model has correctly

identified two class labels. With 70%TRAP, the MHOTL-ECRCD approach offers average $accu_y$ of 95.72%, $prec_n$ of 95.72%, $sens_y$ of 95.72%, $spec_y$ of 95.72%, $F1_{score}$ of 95.65%, and MCC of 91.43%. In addition, with 30%TESP, the MHOTL-ECRCD approach offers average $accu_y$ of 95.66%, $prec_n$ of 95.66%, $sens_y$ of 95.66%, $spec_y$ of 95.66%, $F1_{score}$ of 95.66%, and MCC of 91.32%.
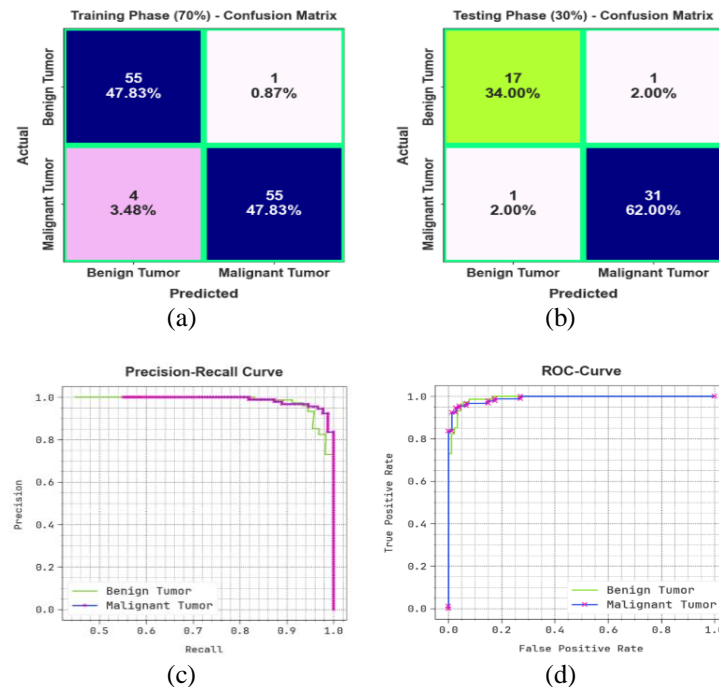

Figure 3. Classifier outcomes of: (a), (b) confusion matrices and (c), (d) curves of PR and ROC

Table 2. CRC detection outcome of MHOTL-ECRCD technique under 70%TRAP and 30%TESP

Class	$Accu_y$	$Prec_n$	$Sens_y$	$Spec_y$	$F1_{Score}$	MCC
TRAP (70%)						
Benign tumor	98.21	93.22	98.21	93.22	95.65	91.43
Malignant tumor	93.22	98.21	93.22	98.21	95.65	91.43
Average	**95.72**	**95.72**	**95.72**	**95.72**	**95.65**	**91.43**
TESP (30%)						
Benign tumor	94.44	94.44	94.44	96.88	94.44	91.32
Malignant tumor	96.88	96.88	96.88	94.44	96.88	91.32
Average	**95.66**	**95.66**	**95.66**	**95.66**	**95.66**	**91.32**

In Figure 4, the training and validation accuracy results from the MHOTL-ECRCD approach are stated. The accuracy outcomes are calculated for 0-25 number of epochs. The figure emphasized that the training and validation accuracy outcomes display a growing tendency that state the capability of the MHOTL-ECRCD approach through enhanced values across different numbers of iterations. Moreover, the training and validation accuracy stays nearer across the number of epochs that designate lower minimal overfitting and demonstrate the higher outcomes of the MHOTL-ECRCD technique, assuring continual prediction on unseen instances.

In Figure 5, the training loss and validation loss graph from the MHOTL-ECRCD methodology is exhibited. The loss results are calculated for 0-25 number of epochs. It is depicted that the training and validation accuracy outcomes indicate a decreasing tendency, which reported the capability of the MHOTL-ECRCD approach in balancing a trade-off between data fitting and generalization. The steady decrease in loss results additionally assurances the greater values of the MHOTL-ECRCD system and tunes the prediction performance over the period. To establish the ability of the MHOTL-ECRCD methodology, a comprehensive comparative analysis is completed in Table 3 [24], [25].
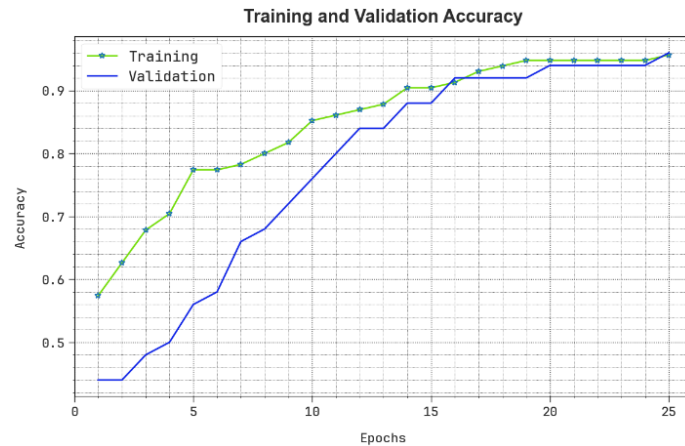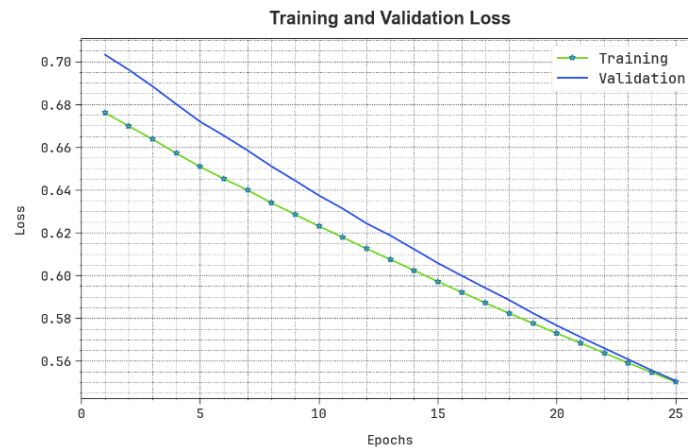
Training and Validation Accuracy

Figure 4. $Accu_y$ curve of the MHOTL-ECRCD technique

Training and Validation Loss

Figure 5. Loss curve of the MHOTL-ECRCD technique

Table 3. Comparative analysis of MHOTL-ECRCD technique with existing approaches

Methodology	$Accu_y$	$Prec_n$	$Sens_y$	$Spec_y$	$F1_{Score}$
MHOTL-ECRCD	95.72	95.72	95.72	95.72	95.65
ResNet-18 Model	92.09	91.39	95.02	84.82	90.81
SC-CNN classifier	81.93	89.13	92.02	93.81	92.82
CP-CNN classifier	87.07	94.20	94.85	84.07	94.74
AAI-CCDC	90.52	93.68	93.91	93.07	91.03
VGG-16 algorithm	81.82	89.31	85.11	89.26	93.27
Inception model	84.46	90.02	91.77	93.92	93.25

In Figure 6, a relative $sens_y$ and $spec_y$ results of the MHOTL-ECRCD method are presented. The outcomes illustrate that the VGG-16 and SC-CNN approaches have exposed poor values of $sens_y$ and $spec_y$. Simultaneously, the Inception and CP-CNN models have gained somewhat better $sens_y$ and $spec_y$. In the meantime, the AAI-CCDC and ResNet-18 techniques have stated nearer values of $sens_y$ and $spec_y$. However, the MHOTL-ECRCD system outcomes in enhanced performance with $sens_y$ and $spec_y$ of 95.72% and 95.72%, individually.

In Figure 7, a comparable $accu_y$, $prec_n$, and $F1_{score}$ outcomes of the MHOTL-ECRCD model are offered. The outcomes point out that the VGG-16 and SC-CNN techniques have revealed poor values of $accu_y$, $prec_n$, and $F1_{score}$. Concurrently, the Inception and CP-CNN techniques have gained marginally enhanced, $accu_y$, $prec_n$, and $F1_{score}$. In the meantime, the AAI-CCDC and ResNet-18 methodology have portrayed adjacent values of $accu_y$, $prec_n$, and $F1_{score}$. However, the MHOTL-ECRCD system outcomes in better performance with $accu_y$, $prec_n$, and $F1_{score}$ of 95.72%, 95.72%, and 96.65%, respectively.
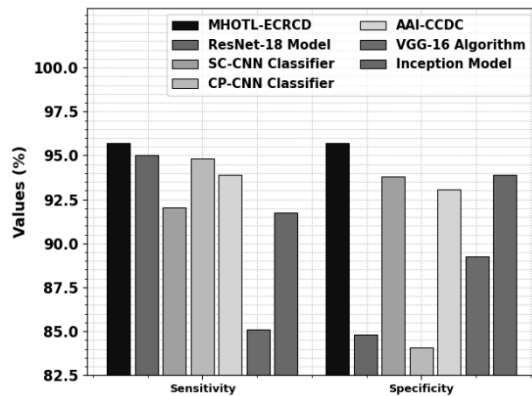
Figure 6. $Sens_y$ and $Spec_y$ analysis of MHOTL-ECRCD technique with existing approaches
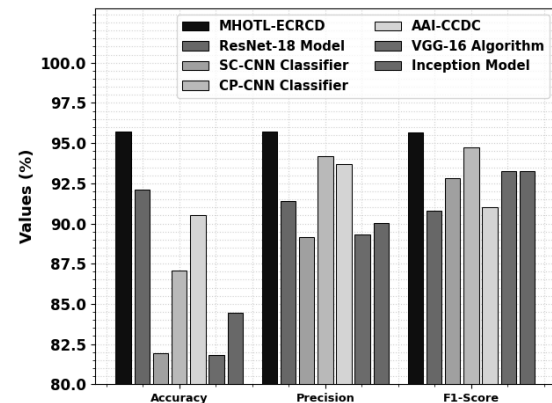

Figure 7. Comparative analysis of MHOTL-ECRCD technique with existing approaches

5.   CONCLUSION

In this article, we have developed a new MHOTL-ECRCD technique. The MHOTL-ECRCD technology mostly concentrates on the classification and detection of CRC utilizing biomedical imaging. It contains four various kinds of stages involving image preprocessing, feature extraction, classification, and parameter selection. Initially, the MHOTL-ECRCD technique takes place ABF model is used for noise reduction. For feature extraction, the MHOTL-ECRCD technique applies the Inception-ResNet-V2 approach for learning the intrinsic and complex features of the image preprocessing. Moreover, the GRU method is used for the classification and detection of the CRC. Finally, the parameter tuning of the GRU technique is performed by the use of HEOA. To demonstrate the good classification outcome of the MHOTL-ECRCD technology, a broad variety of experiments occurs from the benchmark dataset. The extensive comparative results ensured the betterment of the MHOTL-ECRCD technique over the recent methods. In future, delve into the fusion of diverse imaging techniques (such as CT, MRI, and endoscopy) paired with histopathological insights to elevate the precision of detection and deliver a more thorough examination of CRC. Create and execute real-time detection frameworks that harness the suggested optimization and transfer learning strategies for instant clinical use, potentially enhancing patient results through prompt interventions. Examine the amalgamation of explainable AI approaches to shed light on the model's decision-making journey, thus fostering trust and comprehension among medical practitioners and patients alike.

AUTHOR CONTRIBUTIONS STATEMENT

This journal uses the Contributor Roles Taxonomy (CRediT) to recognize individual author contributions, reduce authorship disputes, and facilitate collaboration.

Name of Author	C	M	So	Va	Fo	I	R	D	O	E	Vi	Su	P	Fu
Lova Naga Babu Ramisetti	✓	✓	✓			✓			✓					
Desidi Narsimha Reddy		✓		✓	✓	✓		✓	✓	✓	✓	✓		
HariKrishna Pathipati	✓	✓	✓	✓		✓			✓		✓		✓	
Yenumula Srividya		✓			✓							✓		
Swetha Pesaru					✓		✓	✓		✓		✓		

C	: **C**onceptualization	I	: **I**nvestigation	Vi	: **Vi**sualization
M	: **M**ethodology	R	: **R**esources	Su	: **Su**pervision
So	: **So**ftware	D	: **D**ata Curation	P	: **P**roject administration
Va	: **Va**lidation	O	: Writing - **O**riginal Draft	Fu	: **Fu**nding acquisition
Fo	: **Fo**rmal analysis	E	: Writing - Review & **E**diting		

CONFLICT OF INTEREST STATEMENT
Authors state no conflict of interest.

DATA AVAILABILITY
- The authors confirm that the data supporting the findings of this study are available within the article [www.warwick.ac.uk/fac/sci/dcs/research/tia/glascontest/download].

REFERENCES

[1]   M. Mulenga *et al.*, "Feature extension of gut microbiome data for deep neural network-based colorectal cancer classification," *IEEE Access*, vol. 9, pp. 23565–23578, 2021, doi: 10.1109/ACCESS.2021.3050838.

[2]   D. Albashish, "Ensemble of adapted convolutional neural networks (CNN) methods for classifying colon histopathological images," *PeerJ Computer Science*, vol. 8, p. e1031, Jul. 2022, doi: 10.7717/peerj-cs.1031.

[3]   N. Lorenzovici, E. H. Dulf, T. Mocan, and L. Mocan, "Artificial intelligence in colorectal cancer diagnosis using clinical data: non-invasive approach," *Diagnostics*, vol. 11, no. 3, p. 514, Mar. 2021, doi: 10.3390/diagnostics11030514.

[4]   C. Zhou *et al.*, "Histopathology classification and localization of colorectal cancer using global labels by weakly supervised deep learning," *Computerized Medical Imaging and Graphics*, vol. 88, p. 101861, Mar. 2021, doi: 10.1016/j.compmedimag.2021.101861.

[5]   M. J. Tsai and Y. H. Tao, "Deep learning techniques for the classification of colorectal cancer tissue," *Electronics (Switzerland)*, vol. 10, no. 14, p. 1662, Jul. 2021, doi: 10.3390/electronics10141662.

[6]   M. Ragab, W. H. Aljedaibi, A. F. Nahhas, and I. R. Alzahrani, "Computer aided diagnosis of diabetic retinopathy grading using spiking neural network," *Computers and Electrical Engineering*, vol. 101, p. 108014, Jul. 2022, doi: 10.1016/j.compeleceng.2022.108014.

[7]   S. Mehmood *et al.*, "Malignancy detection in lung and colon histopathology images using transfer learning with class selective image processing," *IEEE Access*, vol. 10, pp. 25657–25668, 2022, doi: 10.1109/ACCESS.2022.3150924.

[8]   J. Fan, J. Lee, and Y. Lee, "A transfer learning architecture based on a support vector machine for histopathology image classification," *Applied Sciences (Switzerland)*, vol. 11, no. 14, p. 6380, Jul. 2021, doi: 10.3390/app11146380.

[9]   M. Ragab and A. F. Nahhas, "Optimal deep transfer learning model for histopathological breast cancer classification," *Computers, Materials and Continua*, vol. 73, no. 2, pp. 2849–2864, 2022, doi: 10.32604/cmc.2022.028855.

[10] E. F. Ohata, J. V. S. das Chagas, G. M. Bezerra, M. M. Hassan, V. H. C. de Albuquerque, and P. P. R. Filho, "A novel transfer learning approach for the classification of histological images of colorectal cancer," *Journal of Supercomputing*, vol. 77, no. 9, pp. 9494–9519, Feb. 2021, doi: 10.1007/s11227-020-03575-6.

[11] Y. Peng and H. Deng, "Medical image fusion based on machine learning for health diagnosis and monitoring of colorectal cancer," *BMC Medical Imaging*, vol. 24, no. 1, Jan. 2024, doi: 10.1186/s12880-024-01207-6.

[12] W. Oswald *et al.*, "Fluorescence excitation-scanning hyperspectral imaging with scalable 2D–3D deep learning framework for colorectal cancer detection," *Scientific Reports*, vol. 14, no. 1, Jun. 2024, doi: 10.1038/s41598-024-64917-5.

[13] L. Tang *et al.*, "A new automated prognostic prediction method based on multi-sequence magnetic resonance imaging for hepatic resection of colorectal cancer liver metastases," *IEEE Journal of Biomedical and Health Informatics*, vol. 28, no. 3, pp. 1528–1539, Mar. 2024, doi: 10.1109/JBHI.2024.3350247.

[14] U. Zidan, M. M. Gaber, and M. M. Abdelsamea, "SwinCup: cascaded swin transformer for histopathological structures segmentation in colorectal cancer," *Expert Systems with Applications*, vol. 216, p. 119452, Apr. 2023, doi: 10.1016/j.eswa.2022.119452.

[15] M. Lalinia and A. Sahafi, "Colorectal polyp detection in colonoscopy images using YOLO-V8 network," *Signal, Image and Video Processing*, vol. 18, no. 3, pp. 2047–2058, Dec. 2024, doi: 10.1007/s11760-023-02835-1.

[16] A. Muneer, S. M. Taib, M. H. Hasan, and A. Alqushaibi, "Colorectal cancer recognition using deep learning on histopathology images," in *2023 13th International Conference on Information Technology in Asia, CITA 2023*, Aug. 2023, pp. 25–30, doi: 10.1109/CITA58204.2023.10262551.

[17] P. Sabol *et al.*, "Explainable classifier for improving the accountability in decision-making for colorectal cancer diagnosis from histopathological images," *Journal of Biomedical Informatics*, vol. 109, p. 103523, Sep. 2020, doi: 10.1016/j.jbi.2020.103523.

[18] P. Bedi, S. B. Goyal, A. S. Rajawat, and M. Kumar, "An integrated adaptive bilateral filter-based framework and attention residual U-net for detecting polycystic ovary syndrome," *Decision Analytics Journal*, vol. 10, p. 100366, Mar. 2024, doi: 10.1016/j.dajour.2023.100366.

[19] T. L. Nikmah, R. M. Syafei, and D. N. Anisa, "Inception ResNet v2 for early detection of breast cancer in ultrasound images," *Journal of Information System Exploration and Research*, vol. 2, no. 2, Jul. 2024, doi: 10.52465/joiser.v2i2.439.

[20] A. A. C. Tanjung, D. R. S. Saputro, and N. A. Kurdhi, "Implementation of the bidirectional gated recurrent unit algorithm on consumer price index data in Indonesia," *Barekeng*, vol. 18, no. 1, pp. 95–104, Mar. 2024, doi: 10.30598/barekengvol18iss1pp0095-0104.

[21] M. Cheng, Q. Zhang, and Y. Cao, "An early warning model for turbine intermediate-stage flux failure based on an improved HEOA algorithm optimizing DMSE-GRU model," *Energies*, vol. 17, no. 15, p. 3629, Jul. 2024, doi: 10.3390/en17153629.

[22] "GLAS contest download," *Warwick University*, [Online]. Available: www.warwick.ac.uk/fac/sci/dcs/research/tia/glascontest/download.

[23] K. Sirinukunwattana, D. R. J. Snead, and N. M. Rajpoot, "A stochastic polygons model for glandular structures in colon histology images," *IEEE Transactions on Medical Imaging*, vol. 34, no. 11, pp. 2366–2378, Nov. 2015, doi: 10.1109/TMI.2015.2433900.

[24] A. S. A. M. AL-Ghamdi and M. Ragab, "Tunicate swarm algorithm with deep convolutional neural network-driven colorectal cancer classification from histopathological imaging data," *Electronic Research Archive*, vol. 31, no. 5, pp. 2793–2812, 2023, doi: 10.3934/ERA.2023141.

[25] T. Sharma *et al.*, "Federated convolutional neural networks for predictive analysis of traumatic brain injury: advancements in decentralized health monitoring," *International Journal of Advanced Computer Science and Applications*, vol. 15, no. 4, pp. 910–923, 2024, doi: 10.14569/IJACSA.2024.0150494.

BIOGRAPHIES OF AUTHORS

Lova Naga Babu Ramisetti 🆔 🔍 SC ⊙ did his Master of Computer Applications from Andhra University. He has around 14 years' experience into business intelligence with financial reporting applications and data management, master data management and reporting. His research interests include data mining, business intelligence, artificial intelligence, machine learning, and data analytics. He can be contacted at email: lova.hyperion@gmail.com.

Desidi Narsimha Reddy 🆔 🔍 SC ⊙ is an accomplished professional with an impressive educational background and extensive experience in the field. He holds a postgraduate degree in machine learning and AI from Purdue University, complemented by an MBA in Finance and Information Systems from MG University. Additionally, he has completed a program on Business Analytics: From Data to Insights from Wharton Management School and is a certified Project Management Professional (PMP) from the PMI Institute. He can be contacted at email: dn.narsimha@gmail.com.

Harikrishna Pathipati 🆔 🔍 SC ⊙ his B. Tech from Madras University. He is a seasoned EPMA/ERP Finance and Master Data and Data Governance expert with over 20 years of experience in EPM/ERP/DWH/BI/ Data Science and Artificial Intelligence and Machine Learning. Had published papers in various reputed journals. He has been part of complex implementation teams consisting of a wide array of Hyperion/Oracle EPM on-premises and cloud solutions, including business modeling, analytic services, planning including workforce and public sector, financial reporting. He is involved with integrating multiple projects with Oracle Financials, HCM with Oracle EPM. He can be contacted at email: hypbiplus@hotmail.com.

Yenumula Srividya 🆔 🔍 SC ⊙ is working as assistant professor in information technology from Vignana Bharathi Institute of Technology with B. E from CBIT, OU and M. Tech from BVRIT, JNTUH. Her area of interests includes data mining, data analysis, big data, machine learning. She can be contacted at email: yenumulasrividya@gmail.com.

Swetha Pesaru 🆔 🔍 SC ⊙ a research scholar in computer science and Engineering from JNTUH, with B.Tech from SRTIST, JNTUH and M. Tech from SRTIST, JNTUH. Her research work is on diabetic retinopathy classification and grading. She is working as Assistant Professor at Vignana Bharathi Institute of Technology, Department of Information Technology, Hyderabad. Her research interests include data mining, machine learning, big data, and internet of things. She is the Member of Hyderabad Deccan ACM Chapter from 2020 and IEEE HYD CIS/GRSS Jt. Chapter. She can be contacted at email: swethareddy09@gmail.com.